Data-driven adaptive trajectory tracking control of unmanned marine vehicles under disturbances and DoS attacks

Li-Ying Hao[1], Huiying Liu[1], Yanli Liu[1], and Yongpeng Weng[1]

[1]Dalian University of Technology Department of Engineering Mechanics

May 10, 2023

Abstract

This article researches the trajectory tracking problem for unmanned marine vehicles (UMVs) with disturbances and under denial-of-services (DoS) attacks in the wireless channel. By applying the partial form dynamic linearization algorithm, an equivalent data-driven model of the UMVs with ocean disturbances is firstly established. And the disturbances are estimated by using extended state observer, which improves the immunity of the UMVs to disturbances in the environment, and the robustness of the UMVs systems is better. It is the first time that the DoS attacks are considered under the data model for UMVs, and a novel data-driven adaptive trajectory tracking control framework is constructed. When the proposed equivalent data model suffers from DoS attacks which follows the Bernoulli distribution, an attack predictive compensation mechanism is devised to relieve the influence of DoS attacks. Based on it, the data-driven adaptive trajectory tracking controller is designed such that the error of trajectory tracking is convergent under DoS attacks and external disturbances. Finally, the effectiveness of the proposed data-driven control scheme and the predictive compensation mechanism is validated through the simulations.

Received: Added at production | Revised: Added at production | Accepted: Added at production

DOI: xxx/xxxx

RESEARCH ARTICLE

Data-driven adaptive trajectory tracking control of unmanned marine vehicles under disturbances and DoS attacks

Huiying Liu | Li-Ying Hao* | Yanli Liu | Yongpeng Weng

Department of Marine Electrical Engineering, Dalian Maritime University, Dalian, China

Correspondence
Li-Ying Hao, Department of Marine Electrical Engineering, Dalian Maritime University, Dalian 116026, China.
Email: haoliying_0305@163.com

Present Address
NO.1, Linghai Road, Dalian 116026, P.R. China

Summary

This article researches the trajectory tracking problem for unmanned marine vehicles (UMVs) with disturbances and under denial-of-services (DoS) attacks in the wireless channel. By applying the partial form dynamic linearization algorithm, an equivalent data-driven model of the UMVs with ocean disturbances is firstly established. And the disturbances are estimated by using extended state observer, which improves the immunity of the UMVs to disturbances in the environment, and the robustness of the UMVs systems is better. It is the first time that the DoS attacks are considered under the data model for UMVs, and a novel data-driven adaptive trajectory tracking control framework is constructed. When the proposed equivalent data model suffers from DoS attacks which follows the Bernoulli distribution, an attack predictive compensation mechanism is devised to relieve the influence of DoS attacks. Based on it, the data-driven adaptive trajectory tracking controller is designed such that the error of trajectory tracking is convergent under DoS attacks and external disturbances. Finally, the effectiveness of the proposed data-driven control scheme and the predictive compensation mechanism is validated through the simulations.

KEYWORDS:
Data-driven control, DoS attacks, trajectory tracking, unmanned marine vehicles

1 | INTRODUCTION

Unmanned marine vehicles (UMVs) have been playing an important role in the field of ocean engineering, including environmental monitoring[1], ocean investigation[2], exploration and development of oil[3] and so on. Thus, achieving operational stability of UMVs is a crucial problem, especially in the areas of dynamic positioning[4], fault-tolerant control[5], mooring control[6] and trajectory tracking control[7], among others.

Trajectory tracking control for UMV model has been an active research area in marine engineering and control areas over the past decades[8–13]. Unfortunately, the UMVs model is not accurate due to the inevitable uncertainties and disturbances caused by harsh ocean environments[8]. The scholars have devoted much effort to model the UMVs and reduce the dependence of algorithms on models. In Reference 9, the authors studied the tracking control problem with parameter uncertainties and unmeasurable state variables. The authors in Reference 10 researched the extended state observers (ESO) by data-driven algorithm for multiple autonomous surface ships. Further more, the authors studied the trajectory tracking control by building data-driven disturbance observers of autonomous surface vehicles in Reference 11. In addition, the authors approximated the nonlinear term in the model by using the radial basis function of underactuated surface vessels in Reference 12. Under the circumstances, the demand for

[0] **Abbreviations:** ANA, anti-nuclear antibodies; APC, antigen-presenting cells; IRF, interferon regulatory factor.

UMVs nominal model seems to be solved, but it remains unsolved when the order of the system model is unavailable. Although the authors address the tracking control problem in Reference 13 by using the proportional-integral-derivative (PID) and fuzzy control approaches, the PID controllers are unable to handle the UMVs nonlinearity. Furthermore, it is hard to determine the parameters of fuzzy controller due to the numerous parameters. Apparently, it is one of critical issues to solve the uncertainty of the model for UMVs. Fortunately, the authors in Reference 14 researched the model-free adaptive control (MFAC), which gives a new direction about it. And the adaptive neural asymptotic tracking control was studied in Reference 15 for networked nonlinear stochastic systems. In Reference 16, the nonlinear time-varying term was estimated by ESO and MFAC algorithm. By using the pseudo-partial derivative (PPD), many equivalent data-driven models were constructed instead of determining the UMVs nonlinear model. The time-varying PPD matrix can be obtained by the plant's input/output (I/O) data. Based on compact form dynamic linearization (CFDL) algorithm, an equivalent dynamic linearization data-driven model for UMVs was built in Reference 17. However, the CFDL method only considers the relationships between the output signal and the input signal in the present moment. Compared with CFDL algorithm, the partial form dynamic linearization (PFDL) algorithm considers it at the preceding L moments [14]. In UMVs system, the change in the output signal at the next moment is not only related to the change in the input signal at the current moment, but also to the previous input signals. Thus, we attempt to build an equivalent dynamical linearization data-driven model of UMVs based on the PFDL algorithm.

It is note that the security of transmission of data is particularly important in UMVs systems, and attacks may lead to disastrous damage of UMVs. The attackers can launch hostile attacks by breaching the integrity of data and destroying the wireless connections among sensors, controllers, and actuators [18]. DoS attacks are one of the common forms of attacks whose purpose is to block or interfere with communication among system components [19]. Hence, the security problem of UMVs subject to DoS attacks began to receive attention. The authors in Reference 20 investigated the secure positioning control problem when a USV under aperiodic DoS attacks. The authors designed an event-triggered mechanism in Reference 21 to mitigate the effects of DoS attacks. The drawback is that the unmanned ocean vehicle was modeled as a linear time-variant system in Reference 20,21. In fact, the dynamic model of UMVs are generally nonlinear. Therefore, the problem of DoS attacks was addressed in Reference 22 for a nonlinear UMV system. But, the control schemes for DoS attacks in Reference 20–22 relied on the model of unmanned ocean vehicle. However, it is hard to build the precise model of UMVs, which may decrease the control performance of the UMVs and bring system instability. Thus, designing a security control scheme for UMVs under DoS attacks without the information of model is a still challenging problem. This promotes us to research a security data-driven control algorithm for UMVs system suffer from DoS attacks.

Motivated by the above analysis, this article studies the data-driven adaptive trajectory tracking problem of UMVs with DoS attacks and external disturbances. The major contributions of this paper are shown:

1. An equivalent data-driven model of UMVs (EDM-UMVs) is first proposed in which disturbances are considered separately. And the disturbances are estimated by ESO. Compared with traditional data-driven model which only considers the I/O data, the EDM-UMVs further considers the effect of external environment disturbances in this paper. It increases the stability of the UMVs and has stronger robustness.

2. Differing from the control scheme proposed in Reference 17, the proposed approach in this paper considers the effect of all input variations within a fixed sliding time window on the output variations at the next moments. A novel PFDL based data-driven adaptive trajectory tracking control (PFDL-DDATTC) algorithm is proposed to achieve the trajectory tracking control for UMVs with external disturbances and DoS attacks in this paper.

3. It is the first time that the DoS attacks are considered for UMVs system under the equivalent data-driven model. A novel data-driven adaptive trajectory tracking control framework is established, and an attack predictive compensation mechanism is designed to compensate the effects of random DoS attacks. The UMV exhibits better tracking performance under DoS attacks with different probabilities of attacks.

The structure of this paper is as follows. Section 2 introduces the problem formulation and relevant preliminaries. In Section 3, the paper introduces the PFDL-DDATTC control scheme and analyzes the convergence of the tracking error system for UMVs under DoS attacks. In Section 4, simulations are conducted to verify the effectiveness of the PFDL-DDATTC algorithm. The conclusion is conducted in Section 5.

2 | PROBLEM FORMULATION AND PRELIMINARIES

Before obtaining an equivalent dynamical linearization data-driven model of UMVs, the UMVs system model is first given as follows[23]:

$$\begin{aligned}\dot{\zeta}(t) &= \boldsymbol{J}(\psi(t))\upsilon(t),\\ \boldsymbol{M}\dot{\upsilon}(t) &= \tau(\upsilon) - N(\upsilon)\upsilon - G(\upsilon)\upsilon - g(\zeta) + \omega(t),\end{aligned} \tag{1}$$

where $\zeta(t) = \begin{bmatrix} x(t) & y(t) & \psi(t)\end{bmatrix}^{\mathrm{T}}$, $(x(t), y(t))$ is the UMVs positions and $\psi(t)$ denotes the yaw angle at instant t; $\upsilon(t) = \begin{bmatrix} \nu(t) & \vartheta(t) & r(t)\end{bmatrix}^{\mathrm{T}}$ expresses the surge velocity , sway velocity and yaw velocity at instant t respectively; $\tau(\upsilon) = \begin{bmatrix}\tau_\nu & \tau_\vartheta & \tau_r\end{bmatrix}^{\mathrm{T}}$ is the control input vector; $g(\zeta) = \begin{bmatrix} g_\nu & g_\vartheta & g_r\end{bmatrix}^{\mathrm{T}}$ is the vector of gravitational/buoyancy forces and moments; $\omega(t) = \begin{bmatrix}\omega_\nu(t) & \omega_\vartheta(t) & \omega_r(t)\end{bmatrix}^{\mathrm{T}}$ represents the disturbances. And $\boldsymbol{J}(\psi(t))$ expresses the rotation matrix with

$$\boldsymbol{J}(\psi(t)) = \begin{bmatrix}\cos(\psi(t)) & -\sin(\psi(t)) & 0\\ \sin(\psi(t)) & \cos(\psi(t)) & 0\\ 0 & 0 & 1\end{bmatrix}.$$

What's more, $\boldsymbol{M}, N(\upsilon), G(\upsilon)$ are unknown in this paper, and it represents the matrices of inertia, coriolis/centripetal force, and damping respectively.

Based on the first-order Euler method and equation (1), it can be derived that:

$$\zeta(n+1) = \zeta(n) + T_s\boldsymbol{J}(\psi(n))\upsilon(n), \tag{2a}$$

$$\upsilon(n+1) = \upsilon(n) + F(n), \tag{2b}$$

where T_s expresses the sampling time, $F(n) = f(\upsilon(n), \zeta(n), \tau(n), \omega(n))$ denotes the unknown dynamics of UMVs with uncertainties and disturbances.

Assumption 1. The disturbances are bounded and exist a positive constant $\bar{\omega}$ so that $\|\omega(n)\| \le \bar{\omega} < \infty$.
Assumption 2. [24] The partial derivative of function $f_i(\cdot), i = 1, 2, 3$ with respect to the input $\upsilon(n), \upsilon(n-1), \cdots, \upsilon(n-L+1)$ is continuous at time n. L is a positive constant, it expresses the length of control input for the UMVs system.
Assumption 3. [24] Define $\Delta\zeta(n) = \zeta(n) - \zeta(n-1), \Delta\upsilon(n) = \upsilon(n) - \upsilon(n-1)$, $\Delta\tau(n) = \tau(n) - \tau(n-1)$, $\Delta\mathcal{T}(n) = \begin{bmatrix}\Delta\tau^{\mathrm{T}}(n) & \Delta\tau^{\mathrm{T}}(n-1) & \cdots & \Delta\tau^{\mathrm{T}}(n-L+1)\end{bmatrix}^{\mathrm{T}}$ and $\Delta\Omega(n) = \begin{bmatrix}\Delta\omega^{\mathrm{T}}(n) & \cdots & \Delta\omega(n-L+1)^{\mathrm{T}}\end{bmatrix}^{\mathrm{T}}$, $\Delta\omega(n) = \omega(n) - \omega(n-1)$, then the UMVs system (2b) satisfies the generalized Lipschitz condition, i.e., $\|\Delta\upsilon(n+1)\| \le \mathcal{L}\|\begin{bmatrix}\Delta\mathcal{T}(n) & \Delta\Omega(n)\end{bmatrix}\|$ for $\forall n$, and $\|\begin{bmatrix}\Delta\mathcal{T}(n) & \Delta\Omega(n)\end{bmatrix}\| \neq 0$, $\|\cdot\|$ denotes Euclidean vector norm.

Assumption 4. For the desired trajectory $\zeta_r(n) = \begin{bmatrix}x_r(n) & y_r(n) & \psi_r(n)\end{bmatrix}^{\mathrm{T}}$, define $\Delta\zeta_r(n) = \zeta_r(n) - \zeta_r(n-1)$, it has $\|\Delta\zeta_r(n)\| \le \mathcal{N}$, where $\mathcal{N}$ is a positive constant.

Remark 1. In practical terms, Assumptions 1-4 of system (2) are reasonable. Assumption 1 restricts the range of disturbances. Assumption 2 describes the classical condition for general nonlinear systems. The variation rate of $\zeta(n)$ was restricted in Assumption 3, which is changed by external disturbances and control input. In terms of energy, the system output is generally bounded due to bounded control input, the same assumption can be seen in Reference 25. Assumption 4 means that the desired trajectory stays in the limited range of the current position of the UMVs.

2.1 | Control Objective

Denote $e(n) = \zeta_r(n+1) - \zeta(n)$ as the error of trajectory tracking of the UMVs system. The control objective for trajectory tracking of the article is to design a data-driven adaptive trajectory tracking control scheme to track the desired trajectory $\zeta_r(n)$ when UMVs suffer from DoS attacks and external disturbances, which can be represented as:

$$\|e(n)\| = \|\zeta_r(n+1) - \zeta(n)\| \le \mathcal{M} \tag{3}$$

where $\mathcal{M}$ is a small positive constant.

3 | MAIN RESULTS

3.1 | PFDL-based equivalent data-driven model with disturbances

In this subsection, the equivalent data-driven model with independent disturbances of UMVs by PFDL algorithm is first given.

Theorem 1. For the UMVs system (2), satisfying Assumptions 1, 2 and 3 with $\|\Delta\mathcal{T}(n)\| \neq 0$, there exist PPD matrices $\bar{\Phi}(n)$ and $\bar{\Psi}(n)$, such that the subsystem (2b) can be converted into an equivalent data-driven model as:

$$\Delta\upsilon(n+1) = \Delta\upsilon(n) + \bar{\Phi}(n)\Delta\mathcal{T}(n) + \bar{\Psi}(n)\Delta\Omega(n), \tag{4}$$

where

$$\bar{\Phi}(n) = \begin{bmatrix}\Phi_1(n) \ \Phi_2(n) \ \cdots \ \Phi_L(n)\end{bmatrix}, \bar{\Psi}(n) = \begin{bmatrix}\Psi_1(n) \ \Psi_2(n) \ \cdots \ \Psi_L(n)\end{bmatrix},$$

$$\Phi_p(n) = \begin{bmatrix}\phi_{11p}(n) & \phi_{12p}(n) & \phi_{13p}(n)\\ \phi_{21p}(n) & \phi_{22p}(n) & \phi_{23p}(n)\\ \phi_{31p}(n) & \phi_{32p}(n) & \phi_{33p}(n)\end{bmatrix}, \Psi_p(n) = \begin{bmatrix}\varphi_{11p}(n) & \varphi_{12p}(n) & \varphi_{13p}(n)\\ \varphi_{21p}(n) & \varphi_{22p}(n) & \varphi_{23p}(n)\\ \varphi_{31p}(n) & \varphi_{32p}(n) & \varphi_{33p}(n)\end{bmatrix},$$

and $p = 1, \cdots, L$, $\|\Phi_p(n)\| \leq \varrho_1$, $\|\Psi_p(n)\| \leq \varrho_2$.

Proof. From equation (2b), we obtain

$$\begin{aligned}\Delta\upsilon(n+1) =& \Delta\upsilon(n) + F(n) - F(n-1)\\ =& \Delta\upsilon(n) + f(\upsilon(n),\zeta(n),\omega(n),\tau(n)) - f(\upsilon(n),\zeta(n),\omega(n),\tau(n-1)) + f(\upsilon(n),\zeta(n),\omega(n),\tau(n-1))\\ &- f(\upsilon(n),\zeta(n),\omega(n-1),\tau(n-1)) + \Xi_1(\upsilon(n),\zeta(n),\omega(n-1),\tau(n-1))\end{aligned} \tag{5}$$

where

$$\Xi_1(\upsilon(n),\zeta(n),\omega(n-1),\tau(n-1)) = f(\upsilon(n),\zeta(n),\omega(n-1),\tau(n-1)) - f(\upsilon(n-1),\zeta(n-1),\omega(n-1),\tau(n-1)).$$

As a matter of fact, the partial derivative of $f(\cdot)$ is related to external disturbance $\omega(n)$, may have two cases: in one case, $\omega(n)$ is continuous smooth function; the other case is that $\omega(n)$ not be differentiable, such as the $\omega(n)$ denotes the time-varying parameters. Therefore, in the following proofs, we will analyze the disturbances in two different situations.

In the first situation, the partial derivative of $f(\cdot)$ related to external disturbance $\omega(n)$ is differentiable, e.g., $\omega(n)$ is continuous smooth function. On the basis of mean value theorem[26] and Assumption 2, one has

$$\Delta\upsilon(n+1) = \Delta\upsilon(n) + \frac{\partial f^*}{\partial\tau_\imath(n)}\Delta\mathcal{T}(n) + \frac{\partial f^*}{\partial\omega_\imath(n)}\Delta\omega(n) + \Xi_1(\upsilon(n),\zeta(n),\omega(n-1),\tau(n-1)), \tag{6}$$

where

$$\frac{\partial f^*}{\partial\tau_\imath(n)} = \begin{bmatrix}\frac{\partial f_1^*}{\partial\tau_{\imath1}(n)} & \frac{\partial f_1^*}{\partial\tau_{\imath2}(n)} & \frac{\partial f_1^*}{\partial\tau_{\imath3}(n)}\\ \frac{\partial f_2^*}{\partial\tau_{\imath1}(n)} & \frac{\partial f_2^*}{\partial\tau_{\imath2}(n)} & \frac{\partial f_2^*}{\partial\tau_{\imath3}(n)}\\ \frac{\partial f_3^*}{\partial\tau_{\imath1}(n)} & \frac{\partial f_3^*}{\partial\tau_{\imath2}(n)} & \frac{\partial f_3^*}{\partial\tau_{\imath3}(n)}\end{bmatrix}, \frac{\partial f^*}{\partial\omega_\imath(n)} = \begin{bmatrix}\frac{\partial f_1^*}{\partial\omega_{\imath1}(n)} & \frac{\partial f_1^*}{\partial\omega_{\imath2}(n)} & \frac{\partial f_1^*}{\partial\omega_{\imath3}(n)}\\ \frac{\partial f_2^*}{\partial\omega_{\imath1}(n)} & \frac{\partial f_2^*}{\partial\omega_{\imath2}(n)} & \frac{\partial f_2^*}{\partial\omega_{\imath3}(n)}\\ \frac{\partial f_3^*}{\partial\omega_{\imath1}(n)} & \frac{\partial f_3^*}{\partial\omega_{\imath2}(n)} & \frac{\partial f_3^*}{\partial\omega_{\imath3}(n)}\end{bmatrix},$$

$$\tau_\imath(n) = \begin{bmatrix}\tau_{\imath1}(n) \ \tau_{\imath2}(n) \ \tau_{\imath3}(n)\end{bmatrix}^{\mathrm{T}}, \tau_{\imath j}(n) = \imath\tau_j(n) + (1-\imath)\tau_j(n-1), j = 1,2,3,$$

$$\omega_\imath(n) = \begin{bmatrix}\omega_{\imath1}(n) \ \omega_{\imath2}(n) \ \omega_{\imath3}(n)\end{bmatrix}^{\mathrm{T}}, \imath \in [0,1], \omega_{\imath j}(n) = \imath\omega_j(n) + (1-\imath)\omega_j(n-1), j = 1,2,3,$$

and $\tau_\imath(n) = [\tau_{\imath1}(n), \tau_{\imath2}(n), \tau_{\imath3}(n)]^{\mathrm{T}}$, $\tau_{\imath j}(n) = \imath\tau_j(n) + (1-\imath)\tau_j(n-1)$, $\omega_\imath(n) = [\omega_{\imath1}(n), \omega_{\imath2}(n), \omega_{\imath3}(n)]^{\mathrm{T}}$, $\omega_{\imath j}(n) = \imath\omega_j(n) + (1-\imath)\omega_j(n-1)$, $j = 1,2,3$. What's more, $\frac{\partial f^*}{\partial\tau_\imath(n)}$ and $\frac{\partial f^*}{\partial\omega_\imath(n)}$ express the value of gradient vector of $f(\cdot)$ with respect to $\upsilon(n), \omega(n)$ at the $\tau_\imath(n)$ and $\omega_\imath(n)$, respectively.

From equation (6), it can be derived that

$$\begin{aligned}\Delta\upsilon(n+1) =& \Delta\upsilon(n) + \frac{\partial f^*}{\partial\tau_\imath(n)}\Delta\mathcal{T}(n) + \frac{\partial f^*}{\partial\omega_\imath(n)}\Delta\omega(n) + \frac{\partial\Xi_1^*}{\partial\tau_\imath(n-1)}\Delta\mathcal{T}(n) + \frac{\partial\Xi_1^*}{\partial\omega_\imath(n-1)}\Delta\omega(n)\\ &+ \Xi_2(\upsilon(n),\zeta(n),\omega(n-2),\tau(n-2)),\end{aligned} \tag{7}$$

where

$$\Xi_2(\upsilon(n),\zeta(n),\omega(n-2),\tau(n-2)) = \Xi_1(\upsilon(n),\zeta(n),\omega(n-1),\tau(n-1)),$$

$$\frac{\partial \Xi_1^*}{\partial \tau_\iota(n-1)} = \begin{bmatrix} \frac{\partial \xi_1^*}{\partial \tau_{\iota 1}(n-1)} & \frac{\partial \xi_1^*}{\partial \tau_{\iota 2}(n-1)} & \frac{\partial \xi_1^*}{\partial \tau_{\iota 3}(n-1)} \\ \frac{\partial \xi_2^*}{\partial \tau_{\iota 1}(n-1)} & \frac{\partial \xi_2^*}{\partial \tau_{\iota 2}(n-1)} & \frac{\partial \xi_2^*}{\partial \tau_{\iota 3}(n-1)} \\ \frac{\partial \xi_3^*}{\partial \tau_{\iota 1}(n-1)} & \frac{\partial \xi_3^*}{\partial \tau_{\iota 2}(n-1)} & \frac{\partial \xi_3^*}{\partial \tau_{\iota 3}(n-1)} \end{bmatrix}, \frac{\partial \Xi_1^*}{\partial \omega_\iota(n-1)} = \begin{bmatrix} \frac{\partial \xi_1^*}{\partial \omega_{\iota 1}(n-1)} & \frac{\partial \xi_1^*}{\partial \omega_{\iota 2}(n-1)} & \frac{\partial \xi_1^*}{\partial \omega_{\iota 3}(n-1)} \\ \frac{\partial \xi_2^*}{\partial \omega_{\iota 1}(n-1)} & \frac{\partial \xi_2^*}{\partial \omega_{\iota 2}(n-1)} & \frac{\partial \xi_2^*}{\partial \omega_{\iota 3}(n-1)} \\ \frac{\partial \xi_3^*}{\partial \omega_{\iota 1}(n-1)} & \frac{\partial \xi_3^*}{\partial \omega_{\iota 2}(n-1)} & \frac{\partial \xi_3^*}{\partial \omega_{\iota 3}(n-1)} \end{bmatrix}.$$

Based on mathematical induction, from equation (7), it has

$$\begin{aligned} \Delta \upsilon(n+1) =& \Delta \upsilon(n) + \left[\frac{\partial f^*}{\partial \tau_\iota(n)} \ \frac{\partial \Xi_1^*}{\partial \tau_\iota(n-1)} \ \cdots \ \frac{\partial \Xi_{L-1}^*}{\partial \tau_\iota(n-L+1)} \right] \Delta \mathcal{T}(n) \\ &+ \left[\frac{\partial f^*}{\partial \omega_\iota(n)} \ \frac{\partial \Xi_1^*}{\partial \omega_\iota(n-1)} \ \cdots \ \frac{\partial \Xi_{L-1}^*}{\partial \omega_\iota(n-L+1)} \right] \Delta \Omega(n) + \Xi_L(\upsilon(n), \zeta(n), \omega(n-L), \tau(n-L)). \end{aligned} \tag{8}$$

Combined with (5), (6) and (7), we get:

$$\Delta \upsilon(n+1) = \Delta \upsilon(n) + \left[\frac{\partial f^*}{\partial \tau_\iota(n)} \ \frac{\partial \Xi_1^*}{\partial \tau_\iota(n-1)} \ \cdots \ \frac{\partial \Xi_{L-1}^*}{\partial \tau_\iota(n-L+1)} \right] \Delta \mathcal{T}(n) + \left[\frac{\partial f^*}{\partial \omega_\iota(n)} \ \frac{\partial \Xi_1^*}{\partial \omega_\iota(n-1)} \ \cdots \ \frac{\partial \Xi_{L-1}^*}{\partial \omega_\iota(n-L+1)} \right] \Delta \Omega(n) + \Gamma(n), \tag{9}$$

where

$$\Gamma(n) = \Xi_L(\upsilon(n), \zeta(n), \omega(n-L), \tau(n-L)).$$

In the other situation, the partial derivative of $f(\cdot)$ is non-differentiable, e.g., $\omega(n)$ changed suddenly at the sampling instant. From (5), in the sampling instant, there exists at least one function $h(\cdot) \in \mathcal{R}^3$ which satisfies Assumptions 1,2, and 3 such that

$$h(\upsilon(n), \zeta(n), \omega(n), \tau(n)) = f(\upsilon(n), \zeta(n), \omega(n-1), \tau(n-1)).$$

Therefore, we can get the equation (9) similarly.

Considering the following equation with variable matrix $\mathcal{H}(n) \in \mathcal{R}^{3\times 3L}$, $\mathcal{A}(n) \in \mathcal{R}^{3\times 3L}$:

$$\Gamma(n) = \mathcal{H}(n)\Delta \mathcal{T}(n) + \mathcal{A}(n)\Delta \Omega(n). \tag{10}$$

Due to $\|\Delta \mathcal{T}(n)\| \neq 0$, there exist $\mathcal{H}^*(n)$ and $\mathcal{A}^*(n)$ satisfying the (10). In practice, the equation have many solutions for each n. Let $\Phi(n) = \left[\frac{\partial f^*}{\partial \tau_\iota(n)} \ \frac{\partial \Xi_1^*}{\partial \tau_\iota(n-1)} \ \cdots \ \frac{\partial \Xi_{L-1}^*}{\partial \tau_\iota(n-L+1)} \right] + \mathcal{H}^*(n)$, $\Psi(n) = \left[\frac{\partial f^*}{\partial \omega_\iota(n)} \ \frac{\partial \Xi_1^*}{\partial \omega_\iota(n-1)} \ \cdots \ \frac{\partial \Xi_{L-1}^*}{\partial \omega_\iota(n-L+1)} \right] + \mathcal{A}^*(n)$, then the equation (4) holds. From equation (5), we can know that $\left[\Phi(n) \ \Psi(n)\right] \left[\Delta \mathcal{T}(n) \ \Delta \Omega(n)\right]^T = \Delta \upsilon(n+1)$. Then, based on the Assumption 3, it can be derived that $\| \left[\Phi(n) \ \Psi(n)\right] \| \leq \mathcal{L}$ and $\|\Phi(n)\| \leq \varrho_1$, $\|\Psi(n)\| \leq \varrho_2$ also can be derived.

The proof is now complete. □

Remark 2. Different from Reference 17, an equivalent data-driven model of UMVs (EDM-UMVs) with disturbances is established. In this paper, the disturbances and input signals have different PPD matrixes $\bar{\Phi}(n)$ and $\bar{\Psi}(n)$. And the traditional data-driven adaptive control methods only consider the I/O data, the EDM-UMVs (4) considers the effect of disturbances in this paper. It increases the immunity of the UMVs and has stronger robustness. If the disturbances are not considered separately, the EDM-UMVs (4) will degrade into the equation (4) in Reference 17.

Remark 3. Obviously, the EDM-UMVs based on PFDL will degenerate into data-driven model on CFDL when $L = 1$. We establish the EDM-UMVs by PFDL algorithm instead of CFDL algorithm. In practice, the change in the output signal of the UMVs system at the next moment is dependent not only on the change in the input signal at the current moment but also on the previous input signals. The controller can not process the state information fully in the first few moments of the UMVs, which leads to the accumulation of residual data. Thus, the PFDL algorithm is more suitable to research the trajectory tracking of UMVs and makes it possible to study various control problems of UMVs more precisely. The UMVs have better tracking performance with the increase of L in a certain range, but the calculation time will increase. Based on the definition of PFDL algorithm, it can be seen that the dimension of PPD matrixes cannot be determined and the equivalent data-driven model cannot be obtained if L is not fixed. Then the parameter L is usually fixed[27–29].

Before designing the adaptive trajectory tracking controller, the variant of the EDM-UMVs is presented as follows.

Corollary 1. For the UMVs system (2), satisfying Assumptions 1, 2 and 3 with $\|\Delta \mathcal{T}(n)\| \neq 0$, the equivalent data-driven model (4) of UMVs can be rewritten as:

$$\hat{\upsilon}(n+1) = \hat{\bar{\Phi}}'(n)\Delta \mathcal{T}(n) + \hat{\Lambda}'(n), \tag{11}$$

with the following updating laws:

$$\hat{\bar{\Phi}}'(n) = \hat{\bar{\Phi}}'(n-1) + [v(n) - \hat{\bar{\Phi}}'(n-1)\Delta\mathcal{T}(n-1) - \hat{\Lambda}'(n-1)]\frac{\beta\Delta\mathcal{T}^{\mathrm{T}}(n-1)}{\alpha + \|\Delta\mathcal{T}(n-1)\|^2}, \tag{12a}$$

$$\hat{\phi}_{ii1}(n) = \hat{\phi}_{ii1}(1), if\ |\hat{\phi}_{ii1}(n)| \leq \epsilon,$$
$$\hat{\Lambda}'(n) = \hat{\Lambda}'(n-1) + \gamma(v(n) - \hat{v}(n)), \tag{12b}$$

where $\hat{\bar{\Phi}}'(n)$ and $\hat{\Lambda}'(n)$ express the estimation value of $\bar{\Phi}'(n)$ and $\Lambda'(n)$, respectively.

Proof: Define the $W(n) = \bar{\Psi}(n)\Delta\Omega(n)$, and $W(n) = \left[w_1(n)\ w_2(n)\ w_3(n)\right]^{\mathrm{T}}$, then equation (4) can be redescribed as follows:

$$v(n+1) = \bar{\Phi}'(n)\Delta\mathcal{T}(n) + \Lambda(n), \tag{13}$$

where $\bar{\Phi}'(n) = [\Phi_1'(n), \cdots, \Phi_L'(n)]$, and $\Phi_p'(n), p = 1, 2, \cdots, L$ is a diagonally dominant matrix, e.g., $\Phi_p'(n) = diag(\phi_{11p}(n), \phi_{22p}(n), \phi_{33p}(n)), \Lambda(n) = \left[\lambda_1(n)\ \lambda_2(n)\ \lambda_3(n)\right]^{\mathrm{T}}$ and

$$\lambda_j(n) = 2v_j(n) - v_j(n-1) + \sum_{i=1}^{3}\sum_{p=1}^{L}\phi_{jip}(n)\Delta\tau_i(n) - \sum_{p=1}^{L}\phi_{jjp}(n)\Delta\tau_j(n) + \omega_j(n), j = 1, 2, 3.$$

In order to estimate matrix $\bar{\Phi}'(n)$, considering the function is as follows:

$$J(\hat{\bar{\Phi}}'(n)) = \|v(n+1) - \hat{\bar{\Phi}}'(n)\Delta\mathcal{T}(n) - \Lambda(n)\|^2 + \alpha\|\hat{\bar{\Phi}}'(n) - \hat{\bar{\Phi}}'(n-1)\|^2,$$

where α is a positive weight coefficient.

Solving $\frac{\partial J(\hat{\bar{\Phi}}'(n))}{\partial\hat{\bar{\Phi}}'(n)} = 0$, further derived as

$$\hat{\bar{\Phi}}'(n) = \hat{\bar{\Phi}}'(n-1) + [v(n) - \hat{\bar{\Phi}}'(n-1)\Delta\mathcal{T}(n-1) - \Lambda(n-1)]\frac{\beta\Delta\mathcal{T}^{\mathrm{T}}(n-1)}{\alpha + \|\Delta\mathcal{T}(n-1)\|^2},$$
$$\hat{\phi}_{ii1}(n) = \hat{\phi}_{ii1}(1), if\ |\hat{\phi}_{ii1}(n)| \leq \epsilon. \tag{14}$$

where $\beta \in (0, 2), \alpha > 0$.

Suppose $\tilde{\bar{\Phi}}'(n) = \hat{\bar{\Phi}}'(n) - \bar{\Phi}'(n)$, then equation (13) can be rewritten as

$$v(n+1) = \hat{\bar{\Phi}}'(n)\Delta\mathcal{T}(n) + \Lambda'(n), \tag{15}$$

where $\Lambda'(n) = \Lambda(n) - \tilde{\bar{\Phi}}'(n)\Delta\mathcal{T}(n)$.

According to the ESO strategy in Reference 24, the unknown term $\Lambda'(n)$ can be derived by

$$\hat{v}(n+1) = \hat{\bar{\Phi}}'(n)\Delta\mathcal{T}(n) + \hat{\Lambda}'(n),$$
$$\hat{\Lambda}'(n) = \hat{\Lambda}'(n-1) + \gamma(v(n) - \hat{v}(n)), \tag{16}$$

where $\gamma = diag(\gamma_1, \gamma_2, \gamma_3), \gamma_j \in (0, 1), j = 1, 2, 3$. The $\hat{v}(n)$ and $\hat{\Lambda}'(n)$ express the estimation value of $v(n)$ and $\Lambda'(n)$, respectively.

And, the equation (14) can be rewritten as:

$$\hat{\bar{\Phi}}'(n) = \hat{\bar{\Phi}}'(n-1) + [v(n) - \hat{\bar{\Phi}}'(n-1)\Delta\mathcal{T}(n-1) - \hat{\Lambda}'(n-1)]\frac{\beta\Delta\mathcal{T}^{\mathrm{T}}(n-1)}{\alpha + \|\Delta\mathcal{T}(n-1)\|^2}.$$

Therefore, the equivalent data-driven model (11) of UMVs with disturbances is hold. ■

Then, combining with equation (2a), yields

$$\zeta(n+1) = \zeta(n) + T_s J(\psi(n))(\hat{\bar{\Phi}}'(n-1)\Delta\mathcal{T}(n-1) + \hat{\Lambda}'(n-1)). \tag{17}$$

To derive the adaptive trajectory tracking control law, the following control criterion function was considered:

$$J(\tau(n)) = \|\zeta_r(n+1) - \zeta(n+1)\|^2 + \kappa\|\tau(n) - \tau(n-1)\|^2,$$

where $\kappa > 0$ denotes the weighting constant.

Solving $\frac{\partial J(\tau(n))}{\partial \tau(n)} = 0$, the adaptive tracking control law can be derived in the following[25]:

$$\begin{aligned}\tau(n) =&\tau(n-1) + \frac{\varsigma_1 T_s J(\psi(n))\hat{\Phi}_1'^{\mathrm{T}}(n)}{\kappa + \|T_s J(\psi(n))\hat{\Phi}_1'(n)\|^2}(\zeta_r(n+1) - \zeta(n) - T_s J(\psi(n))\hat{\Lambda}'(n-1)) \\ &- \frac{\hat{\Phi}_1'^{\mathrm{T}}(n) T_s J(\psi(n)) \sum_{p=2}^{L} \varsigma_p \hat{\Phi}_p'(n)\Delta\tau(n-p+1)}{\kappa + \|T_s J(\psi(n))\hat{\Phi}_1'(n)\|^2},\end{aligned} \tag{18}$$

where $\varsigma_p \in (0, 1), p = 1, \cdots, L$ is a step-size constant.

3.2 | DoS attacks model and predictive compensation scheme

Generally speaking, the system performance might be decreased once the DoS attacks occur, this is because the useful information will be blocked to the control center. If the aggressors launch DoS attacks on the system and cause the parcel dropouts, the control input cannot be created timely, which make control system be unstable and control objective fail. In this article, the controller cannot receive the data packets once DoS attacks occur. Suppose $y(n) = [\upsilon(n); \zeta(n)]$, the data packets will be represented in the following form:

$$y_{att}(n) = \mu(n)y(n), \tag{19}$$

where $\mu(n)$ complies with Bernoulli distribution. DoS attacks are successful when $\mu(n) = 0$, and DoS attacks fail when $\mu(n) = 1$. The successful probability of the DoS attacks can be represented as $P\{\mu(n) = 0\} = 1 - \bar{\mu}$, the failed one $P\{\mu(n) = 1\} = \bar{\mu}$.

Remark 4. Similar to[30],[31] and[32], the constraint of frequency and duration for random DoS attacks is dealt with by the theory of probability. The DoS attacks usually occur in a stochastic manner, which follow Bernoulli distribution in this paper. It means that the attacks are discontinuous. Instead of frequency, the probability is used to represent the occurrence possibility of random DoS attacks. Based on the probability of attacks, the duration for random DoS attacks is limited. In fact, the attackers can only launch intermittent attacks constrained by finite energy on the wireless channel. Thus, it is reasonable to describe the possibility of DoS attacks by using the Bernoulli distribution.

3.2.1 | Predictive compensation scheme

The following assumptions are given to make the predictive compensation algorithm for DoS attacks more practical.

Assumption 5. [33] The delay of data packet in the wireless channel between controller and sensor can be neglected.

The attack signals is limited due to the restricted energy, and the number of subsequent attacks has an upper bound $\bar{q}$.

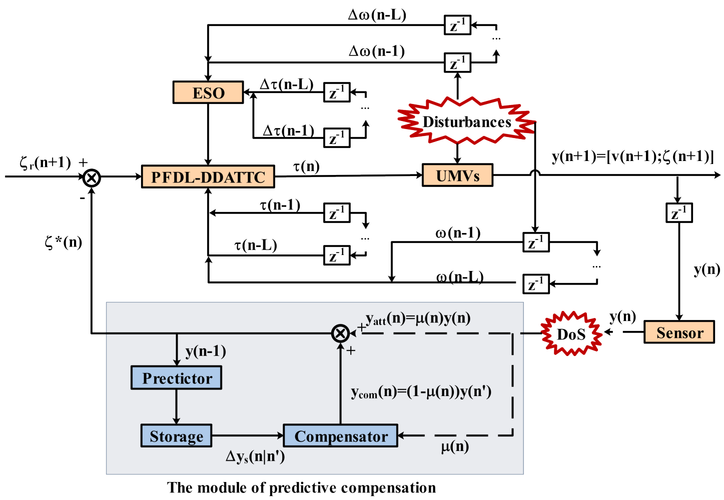

Figure 1 The control structure of the UMVs system against DoS attacks.

From Figure 1, we can see that the module of predictive compensation is embedded to repair the damage caused by the attacks, which composed of a predictor, storage and compensator. The data packet $y(n)$ and $\hat{\hat{\Phi}}'(n)$ will update to $y(n')$ and $\hat{\hat{\Phi}}'(n')$ when the data packet $y(n)$ and $\hat{\hat{\Phi}}'(n)$ are sent to the controller side successfully at time n. Then the predictor will predict a group output data $y(n|n')$ for $n = n' + \imath, \imath = 1, 2, \cdots, \bar{q}$, and store these value of $\Delta\upsilon_s(n|n')$ to storage area. At the same time, the attack signals $\mu(n)$ can be detected. When $\mu(n) = 0$, it means the attackers attack the system successfully, the correspondingly value of $y(n|n')$ in storage will be send to the controller. When $\mu(n) = 1$, the attacks failed, and the predictive compensation does not work. Then, the signals received by PFDL-DDATTC is represented as

$$y(n'|n') = \left[\upsilon^{\mathrm{T}}(n'|n') \ \zeta^{\mathrm{T}}(n'|n')\right]^{\mathrm{T}} \tag{20}$$

So the predictive compensation algorithm is as follows:

$$\Delta\tau(n'|n') = \mathfrak{I}(n')(\zeta_r(n'+1) - \zeta(n'|n') - T_s J(\psi(n'))\hat{\Lambda}'(n'-1)) - \wp(n'), \tag{21}$$

where

$$\mathfrak{I}(n') = \frac{\varsigma_1 T_s J(\psi(n'))\hat{\Phi}_1'^T(n')}{\kappa + \|T_s J(\psi(n'))\hat{\Phi}_1'(n')\|^2}, \wp(n') = \frac{\hat{\Phi}_1'^T(n') T_s J(\psi(n') \sum_{p=2}^{L} \varsigma_p \hat{\Phi}_p'(n')\Delta\tau(n'-p+1)}{\kappa + \|T_s J(\psi(n')\hat{\Phi}_1'(n')\|^2},$$

$\zeta(n'|n') = \zeta(n')$, and $\zeta_r(n'+1)$ is the desired trajectory, which stores in the controller and predictor and can be obtained in advance.

Based on the equation (11), (12), (17), (21), a group of predictive increments for $\imath = 1, 2, \cdots, \bar{q}$ are computed updated as follows:

$$\begin{aligned}
y(n'+\imath|n') &= \left[\upsilon^{\mathrm{T}}(n'+\imath|n') \ \zeta^{\mathrm{T}}(n'+\imath|n')\right]^{\mathrm{T}}, \\
\upsilon(n'+\imath|n') &= \hat{\hat{\Phi}}'(n'-1)\Delta\mathcal{T}(n'+\imath-1|n') + \hat{\Lambda}'(n'-1)), && (22)\\
\upsilon(n'+\imath|n') &= \upsilon(n'+\imath-1|n') + \Delta\upsilon(n'+\imath-1|n'), && (23)\\
\zeta(n'+\imath|n') &= \zeta(n'+\imath-1|n') + T_s J(\psi(n'+\imath|n'))\upsilon(n'+\imath|n'), && (24)\\
\Delta\tau(n'+\imath|n') &= \mathfrak{I}(n')(\zeta_r(n'+1) - \zeta(n'+\imath|n') - T_s J(\psi(n'))\hat{\Lambda}'(n'-1)) - \wp(n'). && (25)
\end{aligned}$$

According to equation (23),

$$\Delta\upsilon_s(n'+\imath|n') = \Delta\upsilon_s(n'+\imath-1|n') + \Delta\upsilon(n'+\imath|n'), \tag{26}$$

where $\Delta\upsilon_s(n'+1|n') = \Delta\upsilon(n'+1|n')$.

From the above the analysis, the corresponding increment sequence as the following:

$$\Delta V_{n'}^{s} = \left[\Delta\upsilon_s^{\mathrm{T}}(n'|n') \ \cdots \ \Delta\upsilon_s^{\mathrm{T}}(n'+\bar{q}|n')\right]^{\mathrm{T}}. \tag{27}$$

When q successive attacks occur after the instant n', the compensator will invoke corresponding $\Delta\upsilon_s(n'+\imath|n')$ from $\Delta V_{n'}^{s}$ for $\imath = 1, 2, \cdots, \bar{q}$, to obtain the compensation value

$$\upsilon(n|n') = \Delta\upsilon_s(n|n') + \upsilon(n'-1). \tag{28}$$

Furthermore, we can obtain that

$$\begin{aligned}
y(n') &= \left[\upsilon^{\mathrm{T}}(n') \ \zeta^{\mathrm{T}}(n')\right]^{\mathrm{T}} \\
\upsilon(n') &= \Delta\upsilon_s(n') + \upsilon(n'-1) = \Delta\upsilon(n') + \upsilon(n'-1), \\
\zeta(n') &= \zeta(n'-1) + T_s J(\psi(n))\upsilon(n'). && (29)
\end{aligned}$$

And there exists a constant c_1 , s.t. $\|\upsilon(n')\| \leq c_1$.

Inspired by Reference 34, we design the attacks compensation mechanism is $y^*(n) = \left[\upsilon^{*\mathrm{T}}(n) \ \zeta^{*\mathrm{T}}(n)\right]^{\mathrm{T}}$, and:

$$\begin{aligned}
\upsilon^*(n) &= \upsilon_{att}(n) + \upsilon_{com}(n) = \mu(n)\upsilon(n) + (1-\mu(n))\upsilon(n'), && (30)\\
\zeta^*(n) &= \zeta(n-1) + T_s J(\psi(n))\upsilon^*(n) = \mu(n)\zeta(n) + (1-\mu(n))\zeta(n').
\end{aligned}$$

Then, based on the predictive compensation mechanism, the resilient controller can be designed in the following:

$$\begin{aligned}\hat{\bar{\Phi}}'(n) =&\hat{\bar{\Phi}}'(n-1) + [v^*(n) - \hat{\bar{\Phi}}'(n-1)\Delta\mathcal{T}(n-1) - \hat{\Lambda}'(n-1)]\frac{\beta\Delta\mathcal{T}^{\mathrm{T}}(n-1)}{\alpha + \|\Delta\mathcal{T}(n-1)\|^2},\\ \hat{\phi}_{ii1}(n) =&\hat{\phi}_{ii1}(1), if\ |\hat{\phi}_{ii1}(n)| \leq \epsilon,\end{aligned} \tag{31a}$$

$$\begin{aligned}\tau(n) =&\tau(n-1) + \frac{\varsigma_1 T_s J(\psi(n))\hat{\Phi}_1'^T(n)}{\kappa + \|T_s J(\psi(n))\hat{\Phi}_1'(n)\|^2}(\zeta_r(n+1) - \zeta^*(n) - T_s J(\psi(n))\hat{\Lambda}'(n-1))\\ &-\frac{\hat{\Phi}_1'^T(n)T_s J(\psi(n))\sum_{p=2}^{L}\varsigma_p\hat{\Phi}_p'(n)\Delta\tau(n-p+1)}{\kappa + \|T_s J(\psi(n))\hat{\Phi}_1'(n)\|^2}.\end{aligned} \tag{31b}$$

Remark 5. Based on the equation (30), it is clear that the compensation mechanism contains two parts, e.g. $y(n)$ and $y(n|n')$. When the $\mu(n) = 0$, namely, the DoS attacks are successful, the controller will use the predictive data $y(n|n')$ for $n = n'+1, \cdots, \bar{q}$ in storage area to reduce the influences of DoS attacks. In the simulations, it is obvious that the compensation scheme improve the trajectory tracking performance largely of systems.

3.3 | Stability analysis

In the subsection, the boundedness of UMVs tracking error systems against DoS attacks is studied. In order to facilitate the subsequent proof, we give the Lemmas in the following.

Lemma 1. [25] Suppose $A = [\alpha_{ij}] \in C^{3\times 3}$, the Gerschgorin disk criterion is expressed as $\mathcal{G}_i = \{r | r - \alpha_{ii}| \leq \sum_{j\neq i,j=1}^{3}|\alpha_{ij}|\}, r \in C, i \in [1,3]$, the Gerschgorin domain $\mathcal{G}_A$ is defined as $\mathcal{G}_A = \bigcup_{i=1}^{3}\mathcal{G}_i$, and all eigenvalues of matrix A exist in $\mathcal{G}_A$.

Lemma 2. [33] Considering the predictive compensation algorithm equation (28), $\Delta v_s(n|n')$ is bounded for $n > n'$.

Before proving the convergence of UMVs tracking error, the analysis of the boundedness of the estimated value of $\bar{\Phi}'(n), \Lambda'(k)$ is given in Corollary 2.

Corollary 2. For system (2), the data-driven model can be written as the equation (11) with the updating laws (12). Considering the DoS attacks signals (19) and the resilient controller (31), the value of $\hat{\bar{\Phi}}'(n)$ and $\hat{\Lambda}'(n)$ are bounded.

Proof. In the initial condition, the conclusion is true.

First, we will prove $\hat{\bar{\Phi}}'(n)$ is bounded.

In one situation, the $\hat{\bar{\Phi}}'(n)$ is bounded when $|\hat{\phi}_{ii}(n)| \leq \epsilon$.

In other situation, $|\hat{\phi}_{ii}(n)| > \epsilon$, from equation (31a), we will have

$$\begin{aligned}\tilde{\bar{\Phi}}'(n) =&[I + (\mu(n)-1)\frac{\beta\Delta\mathcal{T}(n-1)\Delta\mathcal{T}^T(n-1)}{\alpha + \|\Delta\mathcal{T}(n-1)\|^2}]\tilde{\bar{\Phi}}'^T(n-1) + \frac{\beta\Delta\mathcal{T}(n-1)}{\alpha + \|\Delta\mathcal{T}(n-1)\|^2}\bar{\Phi}'(n-1)\\ &+ \frac{\beta\Delta\mathcal{T}(n-1)}{\alpha + \|\Delta\mathcal{T}(n-1)\|^2}(\mu(n)(\Lambda'^T(n-1) - \hat{\Lambda}'^T(n-1))) + \frac{\beta\Delta\mathcal{T}(n-1)}{\alpha + \|\Delta\mathcal{T}(n-1)\|^2}(1-\mu(n))v^T(n') - \Delta\bar{\Phi}'(n).\end{aligned} \tag{32}$$

Taking norm and the exception for (32), one has:

$$\begin{aligned}E\{\|\tilde{\bar{\Phi}}'(n)\|\} \leq&E\{\|I + (\bar{\mu}-1)\frac{\beta\Delta\mathcal{T}(n-1)\Delta\mathcal{T}^T(n-1)}{\alpha + \|\Delta\mathcal{T}(n-1)\|^2}\|\}E\{\|\tilde{\bar{\Phi}}'^T(n-1)\|\}\\ &+ E\{\|\frac{\beta\Delta\mathcal{T}(n-1)}{\alpha + \|\Delta\mathcal{T}(n-1)\|^2}\|\}E\{\|\bar{\Phi}'(n-1)\|\} + \bar{\mu}E\{\|\frac{\beta\Delta\mathcal{T}(n-1)}{\alpha + \|\Delta\mathcal{T}(n-1)\|^2}\|\}E\{\|\tilde{\Lambda}'(n-1)\|\}\\ &+ (1-\bar{\mu})E\{\|\frac{\beta\Delta\mathcal{T}(n-1)}{\alpha + \|\Delta\mathcal{T}(n-1)\|^2}\|\}E\{\|v(n')\|\} + E\{\|\Delta\bar{\Phi}'(n)\|\},\end{aligned} \tag{33}$$

where $\tilde{\Lambda}'^T(n-1) = \hat{\Lambda}'^T(n-1) - \Lambda'^T(n-1)$, and constant d satisfies $\|\tilde{\Lambda}'(n-1)\| \leq d$.

What's more,

$$\|I + (\bar{\mu}-1)\frac{\beta\Delta\mathcal{T}(n-1)\Delta\mathcal{T}^T(n-1)}{\alpha + \|\Delta\mathcal{T}(n-1)\|^2}\|^2 \leq l. \tag{34}$$

where $l \in (0,1)$ is a constant.

Note

$$\|\frac{\beta\Delta\mathcal{T}^T(n-1)}{\alpha+\|\Delta\mathcal{T}(n-1)\|^2}\|=\frac{\beta\|\Delta\mathcal{T}(n-1)\|}{\alpha+\|\Delta\mathcal{T}(n-1)\|^2}=\frac{\beta}{\frac{\alpha}{\|\Delta\mathcal{T}(n-1)\|}+\|\Delta\mathcal{T}(n-1)\|}\leq\frac{\beta}{2\sqrt{\alpha}}. \tag{35}$$

Furthermore, from Theorem 1, we can know $\|\bar{\Phi}'(n)\|\leq\varrho_1$, then

$$\|\Delta\bar{\Phi}'(n)\|\leq 2\varrho_1. \tag{36}$$

Then, substituting (34), (35), (36) into (33) yields

$$E\{\|\tilde{\bar{\Phi}}'(n)\|\}\leq lE\{\|\tilde{\bar{\Phi}}'(n-1)\|\}+c_2, \tag{37}$$

where $c_2=\frac{\beta\varrho_1}{2\sqrt{\alpha}}+\bar{\mu}\frac{\beta d}{2\sqrt{\alpha}}+(1-\bar{\mu})\frac{\beta c_1}{2\sqrt{\alpha}}+2\varrho_1$.

And from (37), we have

$$E\{\|\tilde{\bar{\Phi}}'(n)\|\}\leq lE\{\|\tilde{\bar{\Phi}}'(n-1)\|\}+c_2\leq l^{n-1}E\{\|\tilde{\bar{\Phi}}'(1)\|\}+\frac{c_2}{1-l}.$$

This means $\tilde{\bar{\Phi}}'(n)$ and $\hat{\bar{\Phi}}'(n)$ are bounded.

Second, we will prove the estimation value of $\hat{\Lambda}'(n)$ is bounded.

Suppose $\tilde{\Lambda}'(n)=\hat{\Lambda}'(n)-\Lambda'(n)$ and $\|\tilde{\Lambda}'(n)\|<c_3$ combined with (15) and (16), we have

$$\tilde{v}(n+1)=(I-\gamma)\tilde{v}(n)+\tilde{\Lambda}'(n)-\Delta\Lambda'(n), \tag{38}$$

where $\Delta\Lambda'(n)=\Lambda'(n)-\Lambda'(n-1)$, $c_3>0$ is a constant, $I\in R^3$ is unit matrix.

Considering (15), $\tilde{\bar{\Phi}}'(n)$ and $\Lambda'(n)$ are bounded. And

$$\max\|\Delta\Lambda'(n)\|\leq c_4, \tag{39}$$

where $c_4>0$ is a constant.

Taking norm and the exception for both sides of (38), then yields that:

$$E\{\|\tilde{v}(n+1)\|\}=(I-\gamma)E\{\|\tilde{v}(n)\|\}+c_3+c_4. \tag{40}$$

Integrating equation (40) with (39), we can get

$$E\{\|\tilde{v}(n+1)\|\}\leq\|(I-\gamma)^{n-1}\|E\{\|\Delta\tilde{v}(1)\|\}+(\|(I-\gamma)^{n-1}\|+\cdots+\|I-\gamma\|+\|I\|)(c_3+c_4).$$

Thus, $\tilde{v}(n+1)$ is bounded, it means $\hat{\Lambda}'(n)$ is bounded.

The proof is now complete. □

Theorem 2. For the UMVs system (1), the equivalent data-driven model of UMVs (4) satisfies Assumptions 1, 2, 3 and 4, the resilient controller is given by the PFDL-DDATTC scheme (31) for trajectory tracking $\zeta_r(n)$, then there exists constant $\mathcal{M}$ is as follows:

$$\mathcal{M}=(p_1+p_2)^nE\{\Gamma(1)\}+(p_2p_1\mathcal{N}_7)^n+\mathcal{N}_7, \tag{41}$$

where $p_1+p_2<1$, $\Gamma(1)$ and $\mathcal{N}_7$ are small constants, such that the error of trajectory tracking is convergent under DoS attacks and external disturbances.

Proof. Based on the equation (25), it yields that

$$\Delta\mathcal{T}(n')=\mathcal{B}_1(n')\Delta\mathcal{T}(n'-1)+\varsigma_1\mathcal{C}_1(n')\mathcal{E}_1(n')-\varsigma_1\mathcal{C}_1(n')\mathcal{F}(n'), \tag{42}$$

where

$$\mathcal{B}_1(n')=\begin{bmatrix}-b_2(n')\cdots-b_L(n') & 0\\ I & 0\end{bmatrix}, b_p(n')=\frac{\varsigma_pT_sJ(\psi(n'))\hat{\Phi}_1'^T(n')\hat{\Phi}_p'(n')}{\kappa+\|T_sJ(\psi(n'))\hat{\Phi}_1'(n')\|^2}, p=2,\cdots,L,$$

$$\mathcal{C}_1(n')=\frac{\begin{bmatrix}T_sJ(\psi(n'))\hat{\Phi}_1'^T(n') & 0\\ 0 & 0\end{bmatrix}}{\kappa+\|T_sJ(\psi(n'))\hat{\Phi}_1'(n')\|^2}, \mathcal{E}_1(n')=\begin{bmatrix}\zeta_r(n'+1)-\zeta(n'|n')\\ 0\end{bmatrix}, \mathcal{F}(n')=\begin{bmatrix}T_sJ(\psi(n'))\hat{\Lambda}'(n')\\ 0\end{bmatrix}.$$

From equation (28) and (29), we have

$$\zeta(n)=\zeta(n'-1)+\Delta\zeta_s(n'+q-1|n')+\zeta(n|n')-\zeta(n'+q-1|n')=\zeta(n|n')+\aleph(n). \tag{43}$$

For $n = n' + q$, it follows

$$\begin{aligned}\Delta\zeta_s(n|n') =&(1-(1-T_sJ(\psi(n')\hat{\bar{\Phi}}'(n')\varsigma_1\mathcal{C}_1(n'))^q)(\zeta_r(n')\\ &-\zeta(n'|n'))+T_sJ(\psi(n'))\hat{\bar{\Phi}}'(n')\mathcal{B}_1(n')\sum_{\iota=1}^{n-1}\Delta\mathcal{T}(n'-\iota)+q(T_sJ(\psi(n'))\hat{\Lambda}'(n')\\ &-T_sJ(\psi(n'))\hat{\bar{\Phi}}'(n')\varsigma_1\mathcal{C}_1(n')\mathcal{F}(n')).\end{aligned} \tag{44}$$

Then, we have

$$\begin{aligned}\aleph(n) =&\zeta(n'-1)-\zeta(n'+q-1|n')-(1-T_sJ(\psi(n'))\hat{\bar{\Phi}}'(n')\varsigma_1\mathcal{C}_1(n'))^q(\zeta_r(n')\\ &-\zeta(n'|n'))+T_sJ(\psi(n'))\hat{\bar{\Phi}}'(n')\mathcal{B}_1(n')\sum_{\iota=1}^{q-1}\Delta\mathcal{T}(n'-\iota)+q(T_sJ(\psi(n'))\hat{\Lambda}'(n')\\ &-T_sJ(\psi(n'))\hat{\bar{\Phi}}'(n')\varsigma_1\mathcal{C}_1(n')\mathcal{F}(n')),\end{aligned} \tag{45}$$

where $\zeta(n'-1), \zeta(n'+q-1|n')$ and $\zeta(n'|n')$ are bounded. As we all know, $\hat{\bar{\Phi}}'(n')$ is bounded , $T_sJ(\psi(n'))\hat{\bar{\Phi}}'(n')\varsigma_1\mathcal{C}_1(n') \in (0,1)$, $\hat{\Lambda}'(n')$ is bounded. Hence, there exists an upper bounded $\bar{\aleph}$ such that $\|\aleph(n)\| \le \bar{\aleph}$ for all n.

Substituting (43) into (30) yields

$$\zeta^*(n) = \zeta(n) - (1-\mu(n))\aleph(n). \tag{46}$$

Due to $e(n) = \zeta_r(n+1) - \zeta(n)$, we have

$$\zeta_r(n+1) - \zeta^*(n) = e(n) + (1-\mu(n))\aleph(n). \tag{47}$$

The equation (31b) can be rewritten as

$$\Delta\mathcal{T}(n) = \mathcal{B}_1(n)\Delta\mathcal{T}(n-1) + \varsigma_1\mathcal{C}_1(n)\mathcal{E}(n) - \varsigma_1\mathcal{C}_1(n)\mathcal{F}_2(n) - \varsigma_1\mathcal{C}_1(n)\mathcal{H}_2(n), \tag{48}$$

where

$$\mathcal{E}(n) = \begin{bmatrix} e^T(n) \\ 0 \end{bmatrix}, \mathcal{F}_2(n) = \begin{bmatrix} T_sJ(\psi(n))\hat{\Lambda}'(n) \\ 0 \end{bmatrix}, \mathcal{H}_2(n) = \begin{bmatrix} (1-\mu(n))\aleph(n) \\ 0 \end{bmatrix}.$$

Then we can derived that

$$\mathcal{E}(n+1) = \mathcal{B}_2(n)\mathcal{E}(n) - \mathcal{B}_3(n)\Delta\mathcal{T}(n-1) + \varsigma_1\mathcal{C}_2(n)\mathcal{F}_2(n) + \varsigma_1\mathcal{C}_2(n)\mathcal{H}_2(n) - \mathcal{F}(n) + \mathcal{Y}_r(n), \tag{49}$$

where

$$\mathcal{B}_2(n) = \begin{bmatrix} I - \frac{\varsigma_1 T_s^2 J^2(\psi(n))\Phi_1'(n)\hat{\Phi}_1'(n)}{\kappa + \|T_sJ(\psi(n))\hat{\Phi}_1'(n)\|^2} & 0 \\ 0 & 0 \end{bmatrix}, \mathcal{B}_3(n) = \begin{bmatrix} -b_2'(n) \cdots - b_L'(n) & 0 \\ I & 0 \end{bmatrix},$$

$$b_p'(n') = \frac{\varsigma_p T_s^2 J^2(\psi(n))\hat{\Phi}_1'^T(n)\hat{\Phi}_p'(n)}{\kappa + \|T_sJ(\psi(n))\hat{\Phi}_1'(n)\|^2}, p = 2, \cdots, L, \mathcal{C}_2(n) = \frac{\begin{bmatrix} T_s^2 J^2(\psi(n))\hat{\Phi}_1'(n)\hat{\Phi}_1'^T(n) & 0 \\ 0 & 0 \end{bmatrix}}{\kappa + \|T_sJ(\psi(n))\hat{\Phi}_1'(n)\|^2}, \mathcal{Y}_r(n) = \begin{bmatrix} \Delta\zeta_r(n) \\ 0 \end{bmatrix}.$$

Taking norm and the exception, the equation (49) is represented as:

$$\begin{aligned}E\{\|\mathcal{E}(n+1)\|\} \le& E\{\|\mathcal{B}_2(n)\mathcal{E}(n)\|\} + E\{\|\mathcal{B}_3(n)\Delta\mathcal{T}(n-1)\|\} + \varsigma_1 E\{\|\mathcal{C}_2(n)\mathcal{F}_2(n)\|\}\\ &+ E\{\|\mathcal{F}(n)\|\} + \varsigma_1(1-\bar{\mu})\bar{\aleph}E\{\|\mathcal{C}_2(n)\|\} + E\{\|\mathcal{Y}_r(n)\|\}.\end{aligned} \tag{50}$$

From Reference 25, using Lemma 1, we can know that the following inequations hold :

$$0 < \mathcal{N}_1 \le \frac{T_s^2 J^2(\psi(n))\hat{\Phi}_1'^T(n)\hat{\Phi}_1'(n)}{\kappa + \|T_sJ(\psi(n))\hat{\Phi}_1'(n)\|^2} < 1, s(\mathcal{B}_3(n)) \le 1, s(\mathcal{B}_2(n)) \le 1 - \varsigma_1\mathcal{N}_1 < 1,$$

where $s(\mathcal{B})$ is the spectral radius of matrix $\mathcal{B}$.

Due to $\bar{\Phi}'(n)$,$\hat{\bar{\Phi}}'(n)$,$\Lambda'(n)$ and $\hat{\Lambda}'(n)$ are bounded, there exist constant $\mathcal{N}_2, \mathcal{N}_3, \mathcal{N}_4, \mathcal{N}_5$ such that

$$\|\mathcal{C}_1(n)\| \le \mathcal{N}_2, \|\mathcal{C}_2(n)\| \le \mathcal{N}_3, \|\mathcal{F}_2(n)\| \le \mathcal{N}_4, \|\mathcal{F}(n)\| \le \mathcal{N}_5, \mathcal{N}_1 + \mathcal{N}_2\mathcal{N}_3 < 1.$$

The characteristic equation of $\mathcal{B}_1(n)$ is

$$r^3 det(r^{L-1}I + \sum_{p=2}^{L} r^{L-p}\frac{\varsigma_p \hat{\Phi}_1'^T(n)\hat{\Phi}_n'(n)}{\kappa + \|\hat{\Phi}_1'(n)\|^2}) = 0.$$

And $det(r^{L-1}I + \sum_{p=2}^{L} r^{L-p}\frac{\varsigma_p \hat{\Phi}_1'^T(n)\hat{\Phi}_n'(n)}{\kappa+\|\hat{\Phi}_1'(n)\|^2})$ is a $3(L-1)$-order monic polynomial, which can be rewritten as $r^{3(L-1)}$ $+ \frac{\max_{p=2,\cdots,L}\varsigma_p}{\kappa+\|\hat{\Phi}_1'(n)\|^2}\chi(r)$, where $\chi(r)$ is a $2(L-1)$-order polynomial.

Due to $\bar{\Phi}'(n)$,$\hat{\bar{\Phi}}'(n)$ are bounded, and $s(\mathcal{B}_3(n)) \leq 1$,

$$\frac{\|\chi(r)\|}{\kappa + \|\hat{\Phi}_1'(n)\|^2} \leq \mathcal{N}_6.$$

where $\mathcal{N}_6$ is a positive constant.

Selecting $\max\limits_{p=2,\cdots,L}\varsigma_p$ such that

$$|r|^{3(L-1)} \leq \max_{p=2,\cdots,L}\varsigma_p\mathcal{N}_6 < 1. \tag{51}$$

Based on equation (51), it has

$$s(\mathcal{B}_3(n)) \leq \{\max_{p=2,\cdots,L}\varsigma_p\mathcal{N}_6\} < 1. \tag{52}$$

Based on $\mathcal{B}$, yields

$$\|\mathcal{B}(n)\| < s(\mathcal{B}(n)) + \varepsilon. \tag{53}$$

Combining with equation (52) and (53), it yields

$$\|\mathcal{B}_3(n)\| < s(\mathcal{B}_3(n)) + \varepsilon \leq p_2 < 1, \|\mathcal{B}_2(n)\| < s(\mathcal{B}_2(n)) + \varepsilon \leq p_1 < 1, \tag{54}$$

where $p_1 = \{\max\limits_{p=2,3,\cdots,L}\varsigma_p\mathcal{N}_6\}^{\frac{1}{3(L-1)}} + \varepsilon, p_2 = 1 - \varsigma_1\mathcal{N}_1 + \varepsilon$.

On the basis of equation (48), and define $\|\Delta\mathcal{T}(0)\| = 0$, one has

$$E\{\|\Delta\mathcal{T}(n)\|\} < \varsigma_1\mathcal{N}_2\sum_{\ell=1}^{n} p_1^{n-\ell}E\{\|\mathcal{E}(\ell)\|\} + \frac{(1-p_1^n)\varsigma_1\mathcal{N}_2(\mathcal{N}_4 + (1-\bar{\mu})\bar{\aleph})}{1-p_1}. \tag{55}$$

Similarly, based on the equation (50) and Assumption 4, we have:

$$\begin{aligned} E\{\|\mathcal{E}(n+1)\|\} <& p_2^n E\{\|\mathcal{E}(1)\|\} + \mathcal{N}_3\sum_{\jmath=1}^{n-1} p_2^{n-1-\jmath}p_1E\{\|\Delta\mathcal{T}(\jmath)\|\} \\ &+ \frac{(\mathcal{N} + \mathcal{N}_5 + \varsigma_1(1-\bar{\mu})\bar{\aleph}\mathcal{N}_2\mathcal{N}_3 + \varsigma_1\mathcal{N}_2\mathcal{N}_3\mathcal{N}_4)(1-p_2^{n-1})}{1-p_2}. \end{aligned} \tag{56}$$

From (55) to (56), it easily leads to

$$E\{\|\mathcal{E}(n+1)\|\} \leq E\{\Gamma(n+1)\} + \mathcal{N}_7(n+1), \tag{57}$$

where

$$\begin{aligned} E\{\Gamma(n+1)\} =& p_2^n E\{\|\mathcal{E}(1)\|\} + \varsigma_1p_1\mathcal{N}_2\mathcal{N}_3\sum_{\jmath=1}^{n-1}p_2^{n-1-\jmath}\sum_{\ell=1}^{\jmath}p_1^{\jmath-\ell}E\{\|\mathcal{E}(\ell)\|\}, \\ \mathcal{N}_7(n+1) =& \frac{(1-p_1^n)\varsigma_1\mathcal{N}_2(\mathcal{N}_4 + (1-\bar{\mu}\bar{\aleph}))}{1-p_1}\frac{\varsigma_1p_1\mathcal{N}_2\mathcal{N}_3(1-p_2^n)}{1-p_2} \\ &+ \frac{(\mathcal{N} + \mathcal{N}_5 + \varsigma_1(1-\bar{\mu})\bar{\aleph}\mathcal{N}_2\mathcal{N}_3 + \varsigma_1\mathcal{N}_2\mathcal{N}_3\mathcal{N}_4)(1-p_2^n)}{1-p_2}. \end{aligned}$$

Suppose $p_3 = \varsigma_1\mathcal{N}_2\mathcal{N}_3$, computing $\Gamma(n+2)$ yields

$$E\{\Gamma(n+2)\} \leq p_2E\{\Gamma(n+1)\} + E\{\gamma(n)\}, \tag{58}$$

where $\gamma(n) = p_3p_1^n\|\mathcal{E}(1)\| + p_3p_1^{n-1}\|\mathcal{E}(2)\| + \cdots + p_3p_1^2\|\mathcal{E}(n-1)\| + p_3p_1(\Gamma(n) + \mathcal{N}_7(n))$, and exists a constant $\mathcal{N}_7$, s.t., $\mathcal{N}_7(n) \leq \mathcal{N}_7$.

Due to

$$p_2 = 1 - \varsigma_1 \mathcal{N}_1 + \varepsilon > \varsigma_1(\mathcal{N}_1 + \mathcal{N}_2\mathcal{N}_3) - \varsigma_1\mathcal{N}_1 + \varepsilon = \varsigma_1\mathcal{N}_2\mathcal{N}_3 + \varepsilon > p_3.$$

The $\gamma(n)$ can be derived as

$$\begin{aligned}\gamma(n) <& p_3 p_1^n \|\mathcal{E}(1)\| + p_3 p_1^{n-1}\|\mathcal{E}(2)\| + \cdots + p_3 p_1^2 \|\mathcal{E}(n-1)\| + p_2 p_1 \mathcal{N}_7 + p_2 p_1 \Gamma(n)\\ <& p_3 p_1^n \|\mathcal{E}(1)\| + p_3 p_1^{n-1}\|\mathcal{E}(2)\| + \cdots + p_3 p_1^2 \|\mathcal{E}(n-1)\| + p_2 p_1 \mathcal{N}_7\\ &+ p_2 p_1 (p_2^{n-1}\|\mathcal{E}(1)\| + p_1 \varsigma_1 \mathcal{N}_2 \mathcal{N}_3 \sum_{\jmath=1}^{n-2} p_2^{n-2-\jmath} \sum_{\ell=1}^{\jmath} p_1^{\jmath-\ell}\|\mathcal{E}(\ell)\|)\\ <& p_1 (p_2^n \|\mathcal{E}(1)\| + p_1 \varsigma_1 \mathcal{N}_2 \mathcal{N}_3 \sum_{\jmath=1}^{n-1} p_2^{n-1-\jmath} \sum_{\ell=1}^{\jmath} p_1^{\jmath-\ell}\|\mathcal{E}(\ell)\|) + p_2 p_1 \mathcal{N}_7\\ =& p_1 \Gamma(n+1) + p_2 p_1 \mathcal{N}_7.\end{aligned} \tag{59}$$

Then from (58) and (59), we get

$$E\{\Gamma(n+2)\} < p_2 E\{\Gamma(n+1)\} + p_1 E\{\Gamma(n+1)\} + p_2 p_1 \mathcal{N}_7. \tag{60}$$

Let $\varsigma_p \in (0,1), p = 1, 2, \cdots, L$ such that

$$\{\max_{p=2,3,\cdots,L} \varsigma_p \mathcal{N}_6\}^{\frac{1}{3(L-1)}} < \varsigma_1 \mathcal{N}_1 < 1, 0 < 1 - \varsigma_1 \mathcal{N}_1 + \{\max_{p=2,3,\cdots,L} \varsigma_p \mathcal{N}_6\}^{\frac{1}{3(L-1)}} < 1.$$

From equation (54), it gets that

$$p_1 + p_2 = 1 - \varsigma_1 \mathcal{N}_1 + \varepsilon + \{\max_{p=2,3,\cdots,L} \varsigma_p \mathcal{N}_6\}^{\frac{1}{3(L-1)}} + \varepsilon < 1, \tag{61}$$

Substituting (61) into (60) gives

$$E\{\Gamma(n+1)\} < (p_1 + p_2) E\{\Gamma(n)\} < (p_1 + p_2)^n E\{\Gamma(1)\} + (p_2 p_1 \mathcal{N}_7)^n \tag{62}$$

Moreover, the boundedness of the trajectory tracking error can be derived that

$$E\{\|\mathcal{E}(n+1)\|\} < \mathcal{M} \tag{63}$$

where $\mathcal{M} = (p_1 + p_2)^n E\{\Gamma(1)\} + (p_2 p_1 \mathcal{N}_7)^n + \mathcal{N}_7$ is a small constant, which is affected by the DoS attacks and external disturbances.

The proof is now complete. □

4 | SIMULATION RESULTS

The purpose of the section is to prove the validity and superiority of the proposed PFDL-DDATTC algorithm.

In the simulation, the desired tracking trajectory as the following:

$$\begin{aligned} x_r(n) =& n;\\ y_r(n) =& 5 + sin(0.05 x_r(n));\\ \psi_r(n) =& arctan(x_r(n), y_r(n)).\end{aligned}$$

And the sampling time is 0.01s, the probability of random DoS attacks occurrence is P. The initial conditions are $\zeta(1) = \begin{bmatrix}0 & 4 & 6\end{bmatrix}^{\mathrm{T}}$; $\upsilon(1) = \begin{bmatrix}0.5 & 0.5 & 0.5\end{bmatrix}^{\mathrm{T}}$. The disturbances are $d_v = 0.015(sin(2\pi n))$; $d_\vartheta = 0.05(sin(2\pi n))$; $d_r = 0.01(sin(2\pi n))$. In the PFDL-DDATTC algorithm, the parameters are as follows: $L = 4, \kappa = 0.4, \varsigma = [0.9; 0.9; 0.9; 0.9], \beta = 0.01$, $\alpha = 0.7$. And the initial value of $\hat{\hat{\Phi}}'(n)$ is $\hat{\hat{\Phi}}'(1) = \begin{bmatrix}\hat{\Phi}_1'(1) & \hat{\Phi}_2'(1) & \hat{\Phi}_3'(1) & \hat{\Phi}_4'(1)\end{bmatrix}^{\mathrm{T}}$, $\hat{\Phi}_1'(1) = diag(0.5, 0.5, 0.5)$, $\hat{\Phi}_2'(1) = diag(0.2, 0.2, 0.2)$, $\hat{\Phi}_3'(1) = diag(0.05, 0.05, 0.05)$, $\hat{\Phi}_4'(1) = diag(0.005, 0.005, 0.005)$.

When the UMV system is only affected by the disturbances and not subjected to DoS attacks, the tracked trajectory and desired trajectory are depicted in Figure 2. It is clear that the UMV can track the desired trajectory with estimation algorithm in subgraph (a), and the actual trajectory fits the desired trajectory quiet well. However, the UMV can not track desired trajectory without it in subgraph (b), there is always a gap between desired trajectory and actual trajectory. It is clear that the disturbances estimation algorithm make tracking performances better when the UMV system is affected by the external disturbances.

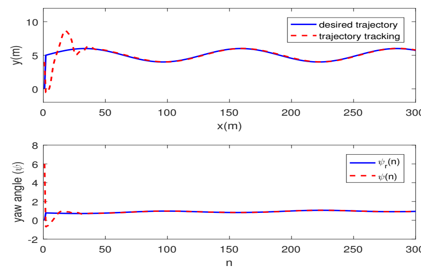

(a) Trajectory-tracking of UMV under disturbances with estimation algorithm.

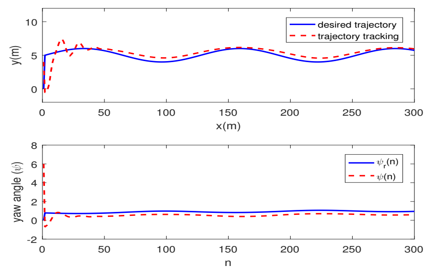

(b) Trajectory-tracking of UMV under disturbances without estimation algorithm.

Figure 2 Comparisons of UMV under disturbances.

When $P = 0.05$, Figure 3 depicts the time response curves for UMV system under DoS attacks without predictive compensation scheme. From Figure 3, the subgraph (a) depicts the tracking performance for trajectory and yaw angle of UMV; subgraph (b) is random variable $\mu(n)$, which represents DoS attacks signals; subgraph (c) denotes the control input signals; subgraph (d) gives the tracking error under the situation. Because of the probability of DoS attacks occurrence is small, the UMV can track the desired trajectory when DoS attacks not occur.

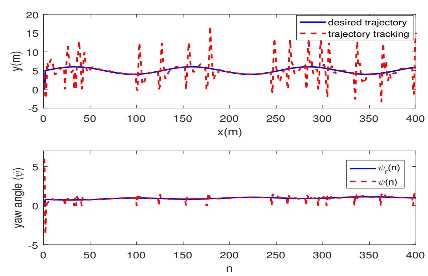

(a) Trajectory-tracking

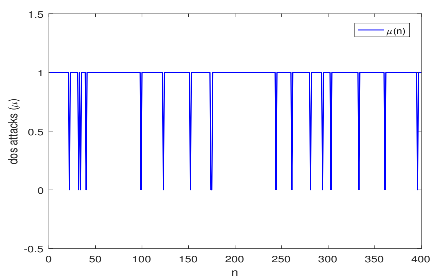

(b) DoS attacks signals

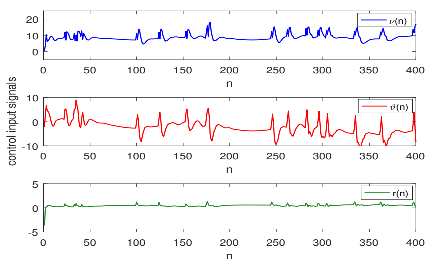

(c) Control input

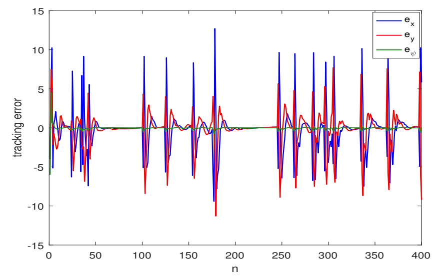

(d) Tracking error

Figure 3 The time response curves of UMV under DoS attacks without predictive compensation with P=0.05.

From Figure 4, it is clear that the tracking performance become worse for UMV with the increase of DoS attacks probability when $P = 0.3$. Without the predictive compensation scheme, the UMV can not track the desired trajectory, and there have larger tracking error. Based on the predictive compensation approach in this article, Figure 5 shows that the UMV can track the desired trajectory when the system under DoS attacks probability is $P = 0.3$. And the UMV can still track the desired trajectory accurately when $P = 0.7$, see Figure 6. The tracking error tends to zero, which shows that the proposed predictive compensation scheme can eliminate the effect of DoS attacks.

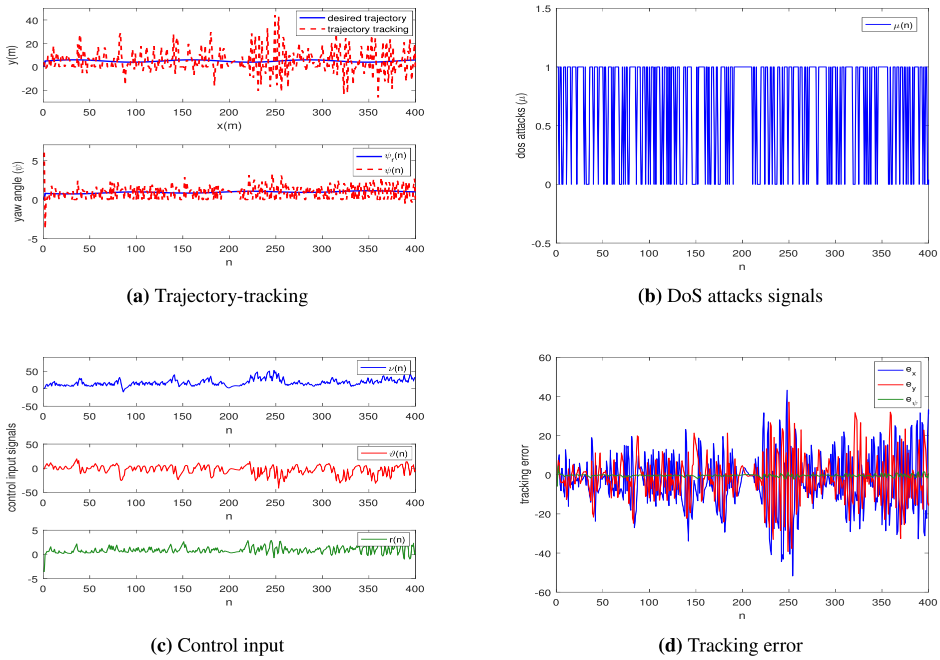

(a) Trajectory-tracking **(b)** DoS attacks signals

(c) Control input **(d)** Tracking error

Figure 4 The time response curves of UMV under DoS attacks without predictive compensation with P=0.3.

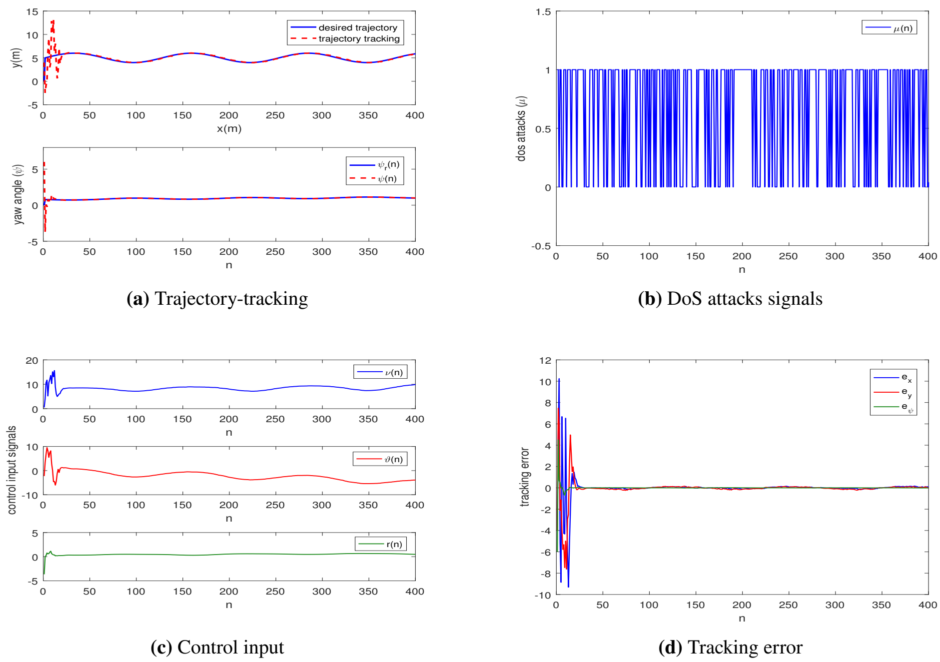

(a) Trajectory-tracking **(b)** DoS attacks signals

(c) Control input **(d)** Tracking error

Figure 5 The time response curves of UMV under DoS attacks with predictive compensation with P=0.3.

In order to indicate the superiority of PFDL-DDATTC algorithm, we make a comparison with the result using the PFDL-DDATTC and CFDL-DDATTC in Reference 17 when P=0.3. The UMV can track the desired trajectory faster under CFDL-DDATTC scheme, but the tracking performance is worse. Compared with CFDL-DDATTC algorithm, the PFDL-DDATTC

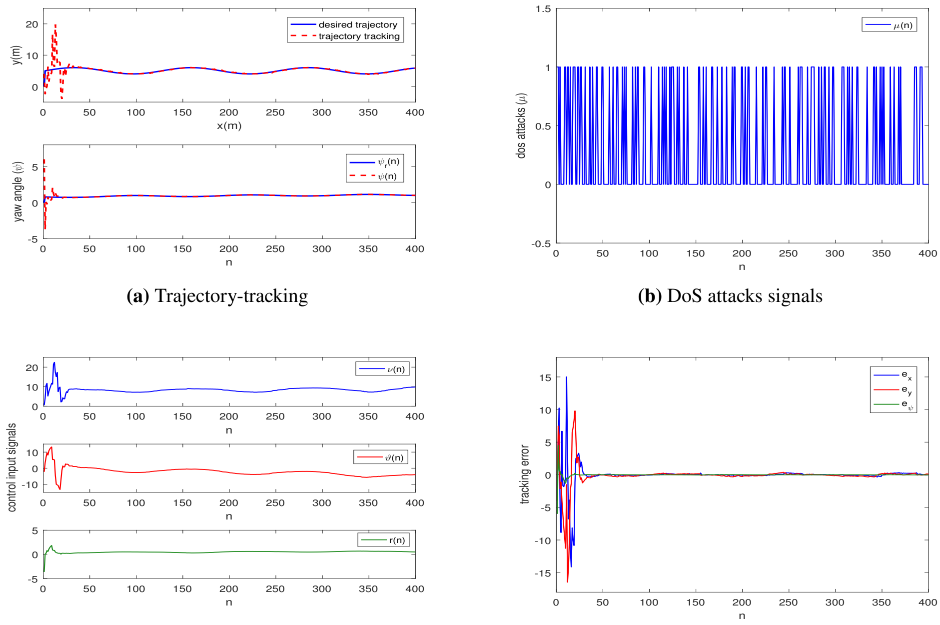

(a) Trajectory-tracking

(b) DoS attacks signals

(c) Control input

(d) Tracking error

Figure 6 The time response curves of UMV system under DoS attacks with predictive compensation with P=0.7.

algorithm ensures the better tracking performance of UMV. It further verifies the effectiveness of the proposed PFDL-DDATTC algorithm.

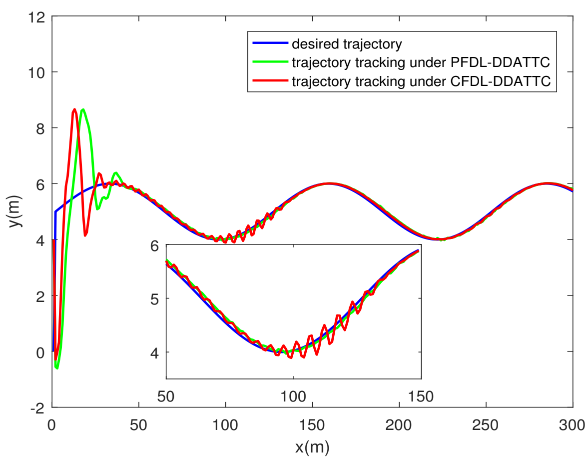

Figure 7 The comparison of trajectory-tracking for UMV under PFDL-DDATTC and CFDL-DDATTC with P=0.3.

5 | CONCLUSION

This paper has studied the problem of data-driven trajectory tracking for UMVs under disturbances and DoS attacks. An equivalent data-driven model has been first proposed which disturbances were considered separately by using PFDL algorithm. And ESO has been used to estimate the disturbances, it increases the immunity of the UMVs to disturbances in the environment and improves the robustness of the controlled system. An effective predicted compensation mechanism has been proposed to eliminate the effectiveness of DoS attacks on control performance. On the basis of EDM-UMVs, a data-driven adaptive trajectory tracking controller with PFDL algorithm has been designed to guaranteed tracking performance for UMVs under DoS attacks. The boundary has been determined for the UMVs trajectory tracking error. Finally, the efficacy of the proposed resilient controller and predicted compensation mechanism in this paper has been demonstrated in the simulations.

ACKNOWLEDGMENTS

This work was supported by the National Natural Science Foundation of China [grant numbers 52171292,51939001]; and the Liaoning Natural Science Foundation Project [grant number 2019-KF-03-09].

Financial disclosure

None reported.

Conflict of interest

The authors declare no potential conflict of interests.

References

1. Moore C, Barnard A, Fietzek P, et al. Optical tools for ocean monitoring and research. *Ocean Science* 2009; 5(4): 661–684. doi: 10.5194/os-5-661-2009

2. Cui W, Wu X. A Chinese strategy to construct a comprehensive investigation system for hadal trenches. *Deep Sea Research Part II: Topical Studies in Oceanography* 2018; 155(9): 27-33. doi: 10.1016/j.dsr2.2018.10.012

3. Cust J, Harding T. Institutions and the location of oil exploration. *Journal of the European Economic Association* 2020; 18(3): 1321–1350. doi: 10.1093/jeea/jvz028

4. Hao LY, Zhang H, Li TS, Lin B, Chen CP. Fault tolerant control for dynamic positioning of unmanned marine vehicles based on TS fuzzy model with unknown membership functions. *IEEE Transactions on Vehicular Technology* 2021; 70(1): 146–157. doi: 10.1109/TVT.2021.3050044

5. Guo G, Li P, Hao LY. Adaptive fault-tolerant control of platoons with guaranteed traffic flow stability. *IEEE Transactions on Vehicular Technology* 2020; 69(7): 6916-6927. doi: 10.1109/TVT.2020.2990279

6. Chen M, Ge SS, How BVE, Choo YS. Robust adaptive position mooring control for marine vessels. *IEEE Transactions on Control Systems Technology* 2013; 21(2): 395-409. doi: 10.1109/TCST.2012.2183676

7. Fetzer KL, Nersesov SG, Ashrafiuon H. Trajectory tracking control of spatial underactuated vehicles. *International Journal of Robust and Nonlinear Control* 2021; 31(10): 4897–4916. doi: 10.1002/rnc.5509

8. Heshmati-Alamdari S, Nikou A, Dimarogonas DV. Robust trajectory tracking control for underactuated autonomous underwater vehicles in uncertain environments. *IEEE Transactions on Automation Science and Engineering* 2021; 18(3): 1288-1301. doi: 10.1109/TASE.2020.3001183

9. Gao Z, Guo G. Command-filtered fixed-time trajectory tracking control of surface vehicles based on a disturbance observer. *International Journal of Robust and Nonlinear Control* 2019; 29(13): 4348–4365. doi: 10.1002/rnc.4628

10. Peng Z, Liu L, Wang J. Output-feedback flocking control of multiple autonomous surface vehicles based on data-driven adaptive extended state observers. *IEEE Transactions on Cybernetics* 2020; 51(9): 4611–4622. doi: 10.1109/TCYB.2020.3009992

11. Peng Z, Wang D, Wang J. Data-driven adaptive disturbance observers for model-free trajectory tracking control of maritime autonomous surface ships. *IEEE Transactions on Neural Networks and Learning Systems* 2021; 32(12): 5584–5594. doi: 10.1109/TNNLS.2021.3093330

12. Liu C, Zou Z, Yin J. Trajectory tracking of underactuated surface vessels based on neural network and hierarchical sliding mode. *Journal of Marine Science and Technology* 2015; 20(2): 322-330. doi: 10.1007/s00773-014-0285-y

13. Dang TS, Duong DT, Le VC, Banerjee S, others . A combined backstepping and adaptive fuzzy PID approach for trajectory tracking of autonomous mobile robots. *Journal of the Brazilian Society of Mechanical Sciences and Engineering* 2021. doi: 10.1007/s40430-020-02767-8

14. Hou Z, Jin S. A novel data-driven control approach for a class of discrete-time nonlinear systems. *IEEE Transactions on Control Systems Technology* 2010; 19(6): 1549–1558. doi: 10.1109/TCST.2010.2093136

15. Li YX, Hu XY, Ahn CK, Hou ZS, Kang HH. Event-based adaptive neural asymptotic tracking control for networked nonlinear stochastic systems. *IEEE Transactions on Network Science and Engineering* 2022; 9(4): 2290-2300. doi: 10.1109/TNSE.2022.3161645

16. Chi R, Hui Y, Zhang S, Huang B, Hou Z. Discrete-time extended state observer-based model-free adaptive control via local dynamic linearization. *IEEE Transactions on Industrial Electronics* 2019; 67(10): 8691–8701. doi: 10.1109/TIE.2019.2947873

17. Weng Y, Wang N, Qin H, Karimi HR, Qi W. Data-driven adaptive tracking control of unknown autonomous marine vehicles. *IEEE Access* 2018; 6: 55723–55730. doi: 10.1109/ACCESS.2018.2872779

18. Yu W, Bu X, Hou Z. Security data-driven control for nonlinear systems subject to deception and false data injection attacks. *IEEE Transactions on Network Science and Engineering* 2022; 9(4): 2910-2921. doi: 10.1109/TNSE.2022.3173310

19. Feng S, Tesi P. Resilient control under denial-of-service: Robust design. *Automatica* 2017; 79: 42–51. doi: 10.1016/j.automatica.2017.01.031

20. Ma Y, Nie Z, Hu S, Li Z, Malekian R, Sotelo M. Fault detection filter and controller co-design for unmanned surface vehicles under DoS attacks. *IEEE Transactions on Intelligent Transportation Systems* 2021; 22(3): 1422-1434. doi: 10.1109/TITS.2020.2970472

21. Fei Z, Wang X, Wang Z. Event-based fault detection for unmanned surface vehicles subject to denial-of-service attacks. *IEEE Transactions on Systems, Man, and Cybernetics: Systems* 2022; 52(5): 3326-3336. doi: 10.1109/TSMC.2021.3064884

22. Ye Z, Zhang D, Cheng J, Wu ZG. Event-triggering and quantized sliding mode control of UMV systems under DoS attack. *IEEE Transactions on Vehicular Technology* 2022; 71(8): 8199-8211. doi: 10.1109/TVT.2022.3175726

23. Zhang C, Cao C, Guo C, Li T, Guo MRc. Navigation multisensor fault diagnosis approach for an unmanned surface vessel adopted particle-filter method. *IEEE Sensors Journal* 2021; 21(23): 27093-27105. doi: 10.1109/JSEN.2021.3122437

24. Weng Y, Gao X. Adaptive sliding mode decoupling control with data-driven sliding surface for unknown MIMO nonlinear discrete systems. *Circuits, Systems, and Signal Processing* 2017; 36(3): 969–997. doi: 10.1007/s00034-016-0353-0

25. Hou Z, Jin S. Data-driven model-free adaptive control for a class of MIMO nonlinear discrete-time systems. *IEEE Transactions on Neural Networks* 2011; 22(12): 2173–2188. doi: 10.1109/TNN.2011.2176141

26. Shen Q, Zhang T. Novel design of adaptive neural network controller for a class of non-affine nonlinear systems. *Communications in Nonlinear Science and Numerical Simulation* 2012; 17(3): 1107–1116. doi: 10.1016/j.cnsns.2011.08.005

27. Chi R, Hui Y, Zhang S, Huang B, Hou Z. Discrete-time extended state observer-based model-free adaptive control via local dynamic linearization. *IEEE Transactions on Industrial Electronics* 2020; 67(10): 8691-8701. doi: 10.1109/TIE.2019.2947873

28. Zhu P, Jin S, Bu X, Hou Z. Improved model-free adaptive control for MIMO nonlinear systems with event-triggered transmission scheme and quantization. *IEEE Transactions on Cybernetics* 2022. doi: 10.1109/TCYB.2022.3203036

29. Hou Z, Jin S. A novel data-driven control approach for a class of discrete-time nonlinear systems. *IEEE Transactions on Control Systems Technology* 2011; 19(6): 1549-1558. doi: 10.1109/TCST.2010.2093136

30. Zhang H, Cheng P, Shi L, Chen J. Optimal denial-of-service attack scheduling with energy constraint. *IEEE Transactions on Automatic Control* 2015; 60(11): 3023–3028. doi: 10.1109/TAC.2015.2409905

31. Zhang H, Cheng P, Shi L, Chen J. Optimal DoS attack scheduling in wireless networked control system. *IEEE Transactions on Control Systems Technology* 2015; 24(3): 843–852. doi: 10.1109/TCST.2015.2462741

32. Ma YS, Che WW, Deng C, Wu ZG. Distributed model-free adaptive control for learnning nonlinear mass under DoS attacks. *IEEE Transactions on Neural Networks and Learning Systems* 2021. doi: 10.1109/TNNLS.2021.3104978

33. Qiu X, Wang Y, Xie X, Zhang H. Resilient model-free adaptive control for cyber-physical systems against jamming attack. *Neurocomputing* 2020; 413: 422–430. doi: 10.1016/j.neucom.2020.04.043

34. Wang Y, Qiu X, Zhang H, Xie X. Data-driven-based event-triggered control for nonlinear CPSs against jamming attacks. *IEEE Transactions on Neural Networks and Learning Systems* 2022; 33(7): 3171-3177. doi: 10.1109/TNNLS.2020.3047931

□